

Horizontally Polarized Antenna Array for an Airborne Ka-PolInSAR System

Alicja Schreiber¹, Markus Limbach¹, Bernd Gabler¹, Andreas Reigber¹

¹ Microwaves and Radar Institute, German Aerospace Center (DLR), Oberpfaffenhofen, Germany, Alicja.Schreiber@dlr.de

Abstract—This paper presents a design of a horizontally polarized antenna array for a new DLR airborne Ka band synthetic aperture radar system with the maximum gain of 24 dB, low cross-pol level of 40 dB and a shaped radiation pattern with low sidelobe level in both azimuth and elevation planes below -18 dB. It has been designed using the slotted waveguide antenna (SWA) technology for the center frequency equal to 35.5 GHz. The transverse slots have been cut into the narrow waveguide wall and the use of iris pairs placed inside enable the radiation. A suitable feeding network consisting of a conventionally H-plane T junction power divider and a directional waveguide coupler has been also described. Based on theoretical principles, the antenna array as well as the corresponding power splitter have been developed and fabricated while meeting mechanical and electrical system demands. The measurement results of the manufactured prototype have been presented and a good agreement with requirements has been achieved.

Index Terms—Slotted Waveguide Antenna, non-inclined slot, polarimetric interferometry, airborne SAR system.

I. INTRODUCTION

The Microwaves and Radar Institute from the German Aerospace Center plays a key role in the development of synthetic aperture radar (SAR) systems. One of them is F-SAR [1], an airborne SAR platform, which is an instrument to verify the new measurement techniques for the future space missions. F-SAR is able to operate up to four different frequencies simultaneously and due to this method, it is possible to gain various information about flown area. It consists currently of seven fully polarimetric antennas operating in five frequency bands: from P band ($f_{0P} = 435$ MHz) up to X band ($f_{0X} = 9.6$ GHz). As the Ka band has gained more and more interest in recent years, the F-SAR system has been expanded to include this frequency band. Due to its short wavelength it has the advantage of developing a relatively compact SAR sensors. Thus, single pass interferometry can be realized more easily and already with small baselines a very good high resolution can be obtained.

The new Ka band system is called Ka-PolInSAR and it is used for polarimetric interferometric SAR measurements. It works in a bistatic configuration consisting of two transmit and up to four receive broadside antennas mounted in side looking mode with an incident angle of 40° . This new SAR system will mainly be applied in snow areas to get information about the structure of the upper snow cover as well as to get

access to biophysical parameters such as snow-water equivalent or firn lines in high mountains glaciers.

The antenna used for this SAR system is developed to operate at the center frequency $f_0 = 35.5$ GHz and it should work within the frequency bandwidth of $B = 0.5$ GHz. To avoid the ambiguities in SAR image, it is necessary to keep sidelobe level (SLL) low in both azimuth and elevation planes, as well as to suppress nadir echo and opposite swath. In Table I all important required values for the final antenna array are summarized.

TABLE I. THE ANTENNA ARRAY REQUIRED PARAMETERS

Antenna Array Specifications		
Parameter	Value	Description
f_0 (GHz)	35.5	Center frequency
B (GHz)	0.5	Bandwidth
G (dB)	~ 20	Gain
θ_{HPBW}/Az ($^\circ$)	$4.5 \div 5$	Half power beam width in azimuth plane
θ_{HPBW}/El ($^\circ$)	$20 \div 25$	Half power beam width in elevation plane
SLL (dB)	< 18	Sidelobe level
Cross-pol (dB)	-40	Cross polarization level

II. ANTENNA DESIGN

The schematic model of the dual polarized Ka band antenna array used for Ka-PolInSAR system is illustrated in Fig. 1.

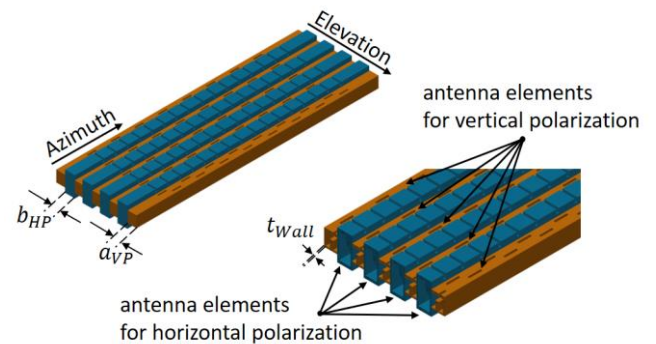


Fig. 1. The model of a dual polarized antenna array used for the Ka-PolInSAR system.

It consists of separate vertically and horizontally polarized antenna elements arranged alternately to each other. The Ka band antenna array described in this paper is a part of it and it is used for creating a horizontally polarized (HP) electric field. The development of the single antenna element for the vertical polarization is not presented in this paper.

A. Single Antenna Element

A single antenna element, from which the antenna array introduced here consists, is built in slotted waveguide antenna technology [2], [3]. This method provides with high power capability, low losses and robust mechanical behavior. If no dielectric material is used, it enables also a maximum possible gain.

SWAs are basically waveguides with slots cut either in broad or narrow wall. The slots must be inserted in such a way, that the interruption of the current flow occurs or an additional structure is needed to achieve this process. Every slot act as a single element. Therefore, by combining several of them, the antenna array theory must be fulfilled.

Since is not necessary to electrically steer the beam, the elements of the same polarization need to be placed with the distance to each other less than the free space wavelength $\lambda_0 = 8.4$ mm in order to obtain a grating lobe free far field pattern. To meet this requirement both the vertical and horizontal waveguides must be modified in such a way, that only the dominant mode TE_{10} is propagated within the desired frequency range. Therefore, the waveguide for generating a horizontal polarization becomes narrower and instead of the standard Ka band waveguide WR28 width of $b_{WR28} = 3.556$ mm, the dimension is $b_{HP} = 2.9$ mm. Whereas the vertical polarized element is built up as a single ridge waveguide with following dimensions $a_{VP} = 3.1$ mm and $b_{VP} = 3.556$ mm. The wall thickness is set to $t_{wall} = 0.5$ mm in both cases. The resulting distance between two elements the same polarization is therefore $0.83 \lambda_0$. The model of the dual polarized configuration is depicted in Fig. 1.

The antenna element is fed centrally by using conventionally H-plane T-junction [4], [5]. The use of this approach enables to create a stable radiation pattern over the desired frequency band. The slotted waveguide antennas with a side feed on the other hand cause the beam steering over the frequency. The SWA here presented is built in standing wave configuration, where the short termination is located a quarter guided wavelength $\lambda_g/4$ away from the last slot. This solution is easy to manufacture and the bandwidth, which is normally slightly narrower compared to the travelling wave mode, is sufficient for this application. The input impedance matching for the H-plane T-junction can be done by changing the position and size of the pin as well as by modifying the dimensions of the insets, which are placed on both sides of the input waveguide as shown in Fig. 2a.

For the horizontally polarized SWA, the slots are typically cut inclined in the narrow wall of the waveguide [6], [7]. From the manufacturing point of view this method is more feasible to realize, but on the other hand the cross-pol level is relatively high, which is undesired for this application. Therefore, the

slots for the antenna here introduced are placed orthogonal to the longitudinal side of the waveguide to overcome this issue. However, as already mentioned, the additional structure is needed to break the current flow, because the transverse slots are parallel to it.

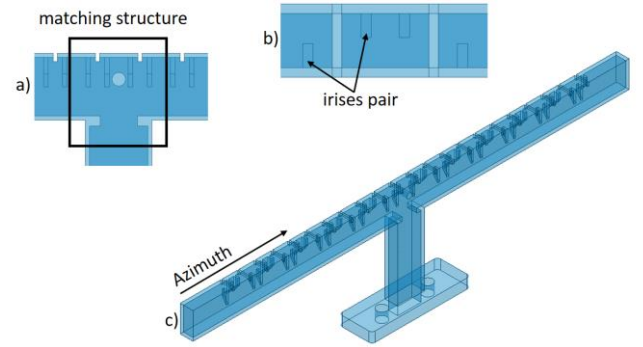


Fig. 2. The simulated model of a single antenna element. a) Matching structure for uniform H-plane T-junction. b) The configuration of used iris pairs. c) The SWA element - side view.

Thus, the iris pairs are used and placed alternately on both sides of each slot to ensure the generation of the equal phase radiated field [8], [9], [10], [11], as seen in Fig. 2b.

The irises act as an obstacle to the current flow causing the slot to radiate. The impedance matching in this configuration can be done by modifying the geometrical dimensions of the iris (length and width) as well as by adjusting the slot length to the desired frequency.

The single antenna element needs to have as low SLL as possible in both planes. It is therefore necessary to implement an amplitude tapering. For the azimuth plane, a \cos^2 -amplitude distribution has been applied. The power radiated through the slot can be controlled by changing the position of the iris pair regarding to the slot as well as by modifying its length.

The final antenna element used for horizontal polarization is composed of 22 slots in order to achieve both the desired half power beam width (θ_{HPBW}/Az) and a shaped radiation pattern with low SLL. A simulation model has been developed and optimized using a 3D electromagnetic field simulator Ansys HFSS as it is depicted in Fig. 2c.

The antenna element, as well as the antenna array have been made from alumina using the erode technology. Since the antenna design is very complex, it was no possible to manufacture the antenna as a single piece. Thus, the antenna array consists of several parts connected by means of a welding device.

B. Antenna Array

The horizontally polarized antenna array consists of four single antenna elements, which is required to meet both the conditions of the desired half power beam width (θ_{HPBW}/El) and a shaped radiation pattern in elevation plane at the same time. In Fig. 3 the manufactured prototype of the antenna array and the single antenna element are illustrated. As here

depicted, the vertical polarized antenna elements are replaced by dummies to create as real environment as possible for the developed HP antenna array.

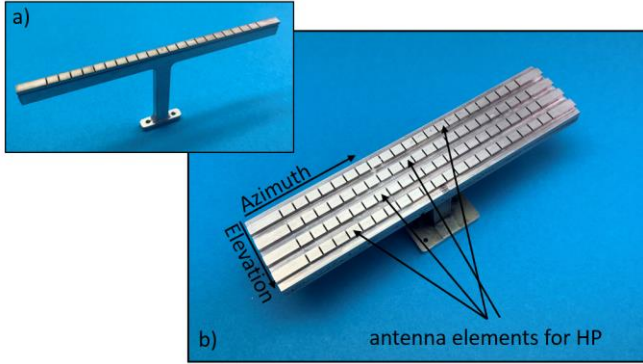


Fig. 3. The fabricated horizontally polarized prototype. a) The single antenna element. b) The antenna array.

C. Feeding Network

Since the radiation pattern for elevation plane must be shaped, a corresponding feeding network with an amplitude distribution is needed. In order to generate a desired far field diagram, the power ratio of 1:5:5:1 is applied. It means, a symmetric amplitude distribution over the four elements is required. A feeding network with two sections is designed and fabricated to meet this condition.

The first section is built as a uniform H-Plane T-junction divider, which splits the incoming power equally to the both output ports. The use of three insets is applied to match the divider at the input, as it can be seen in Fig. 3a. This process can be controlled by changing both the dimensions of the inset placed symmetrically in the output waveguide and two the same size insets located in the input waveguide. Since the waveguide output ports has been changed from H-plane at the input to the E-plane at the output, the phase shift between two output ports of 180° is generated.

The second section is built up as a directional waveguide coupler [13], [14], which has a single rectangle hole placed in the common broad wall between two waveguides. In Fig. 3b the coupler configuration is illustrated. Port 1, 2, 3 and 4 correspond to input, output, coupled and isolated port respectively. The coupling slot is placed centered and its position as well as its geometrical dimensions influence the coupling intensity and the input impedance matching. The four output ports must be placed with the respectively distance to each other, which is as already mentioned 7 mm. The generation of a boresight radiation assumes the same phase output signals. Since both the T-junction and the coupler create the phase shift between the output ports, an additional phase balancing element has been designed to solve this issue. The phase compensation is done by using different waveguide lengths, as illustrated in Fig. 3c. Since the waveguide dimensions for the Ka band SAR system here presented are different to the standard waveguide WR28, a suitable transition has been designed to overcome this issue.

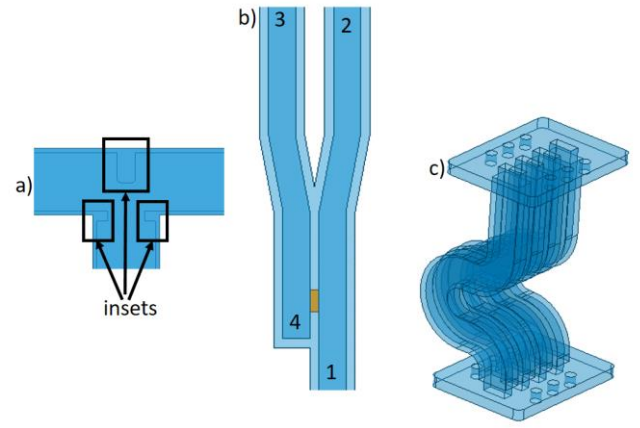


Fig. 4. a) The marked matching structure of the H-plane T-junction. b) The directional waveguide coupler. c) The phase balancing element.

The design based on the theoretical principles has been developed and simulated in order to achieve the desired split ratio. The final feeding network has been manufactured in the same way as the antenna array using the erode technology. The antenna and the feeding network have been fabricated separately in order to get more flexibility. Thus, if a different amplitude distribution for elevation plane is required in the future, only that part must be new designed and manufactured. In Fig. 5 the fabricated feeding network with phase balancing element is presented.

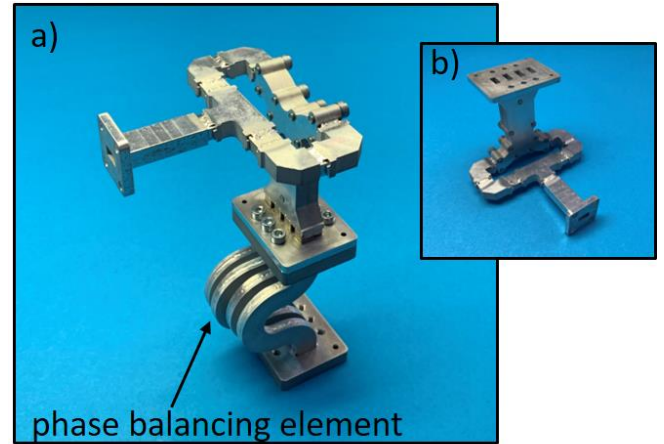


Fig. 5. The fabricated final feeding network. a) The assembly with the phase balancing element. b) The feeding network.

III. MEASUREMENT

The measurements of the manufactured feeding network and the assembly with the antenna array have been done and the achieved results are presented in the following sections.

A. Feeding Network

In Fig. 6 the simulated and measured power divider parameters have been plotted. As it can be seen in the upper diagram, the manufactured feeding network is well matched

over the desired frequency range (marked area), where the reflection coefficient is within this sector below the value of -15 dB. However, the differences between the achieved (solid line) and simulated (dashed line) values can be clearly seen and have been occurred probably due to the manufacturing tolerances and the measurement setup. Since the antenna here presented consists of several elements, the assembly process is a source of potential error. Because of its short wavelength, the antenna reacts very sensitively to manufacturing tolerances, where only small differences can disturb antenna functionality. The use of additional adapters during the measurement increases the probability of having an incorrect match at the input too.

The required power ratio has been achieved as well, which is illustrated in the lower diagram. The measured values (solid lines) shown little deviations compared to the simulated data (dashed lines). The transmitted signal at two outer ports have approximately 7 dB less power than the signal coming to the inner ports. As in this diagram depicted, the values remain at a similar level over required frequency range, which is an important approach to having a stable radiation pattern.

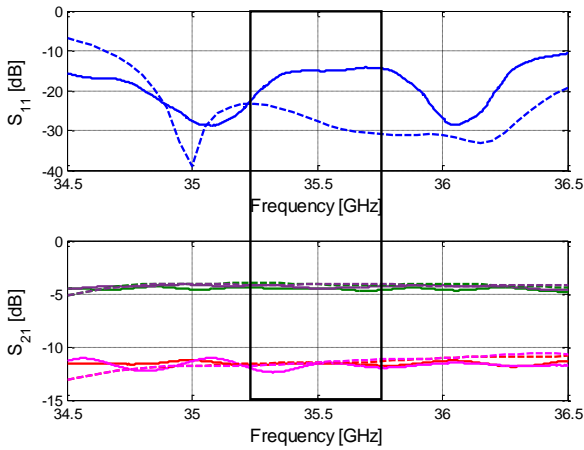


Fig. 6. The simulated (dashed line) and measured (solid line) reflection coefficient (upper diagram) and transmission coefficient (lower diagram) of the feeding network. The marked area shown the required frequency range.

B. Antenna Array

The antenna array with the feeding network has been measured in the DLR's Compact Test Range (CTR) [15]. As illustrated in Fig. 7 the antenna input is well matched over the required frequency band from 35.25 GHz up to 35.75 GHz. The measured reflection coefficient (solid line) is below -15 dB in the entire range and shows a very good agreement with the simulation results (dashed line).

In Fig. 8 both the simulated and measured radiation pattern in the azimuth plane have been illustrated. The antenna beam should have a narrow shape in this plane and as it can be seen from this diagram this condition has been met, where the half power beam width is equal to 4.7° for the center frequency. The demand on having low SLL has been obtained as well. The first sidelobe is 18 dB below the main lobe. The achieved total gain is equal to 23.7 dB, which fulfill the requirement.

The measurement results agree well with simulations and slight differences can be attributed to the phase discrepancies, which achieved due to the manufacturing tolerances.

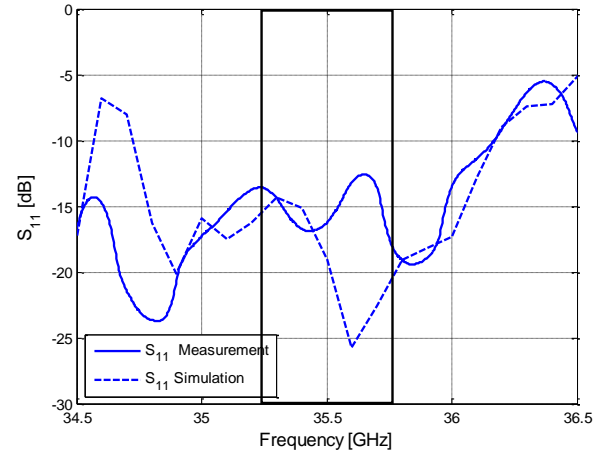


Fig. 7. The measured (solid line) and simulated (dashed line) reflection coefficient of the final antenna array. The marked area shown the required frequency range of 35.25 GHz - 35.75 GHz.

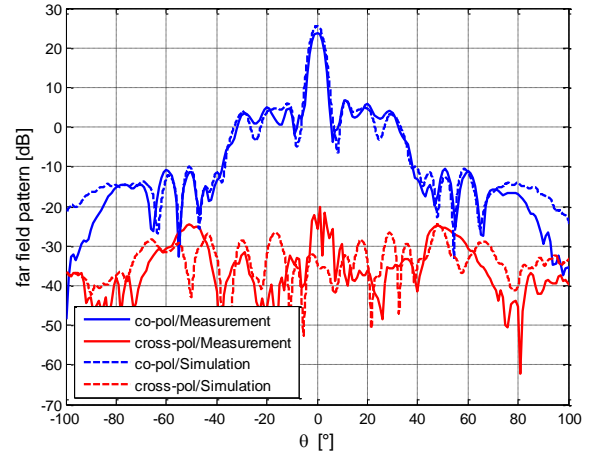


Fig. 8. The measured and simulated co- and cross - polarization far field pattern of the final antenna array for the center frequency $f_0=35.5$ GHz in azimuth plane.

In Fig. 9 the co - and cross - polarization far field pattern for the center frequency in the elevation plane has been plotted, both simulated and measured. The achieved SLL is lower than 18 dB under the main lobe while the cross-polarization level is located approximately 40 dB under the main lobe.

An important requirement for airborne systems with side-looking antennas is to generate a radiation pattern in the elevation plane with both nadir echo as well as opposite swath suppressed. Nadir describes in this case the direction that is perpendicular to the antenna's azimuth axis and in side looking mode as here used forms the shortest way back of the receive signal. In the SAR systems using this configuration strong backscattered nadir echo can lead to generation of ambiguities

in SAR image. The antenna here presented is mechanically steered and get the maximum at 40° , as shown in Fig. 9. Thus, it is necessary to create a null at that point. The same counts for opposite swath, which represent the area located opposite to the generated radiation diagram and it should have low backscattered signal. As in Fig. 9 depicted, these two conditions have been met well.

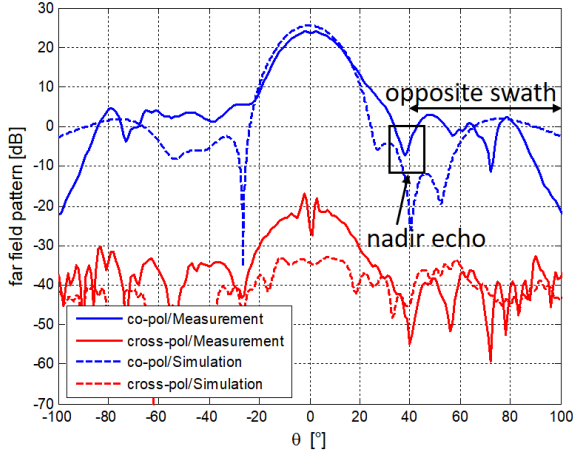


Fig. 9. The measured and simulated co- and cross - polarisation far field pattern of the final antenna array for the center frequency $f_0=35.5\text{GHz}$ in elevation plane.

In order to have a statement about the functionality of the antenna over the desired frequency band, antenna gain and half power beam width for both azimuth and elevation planes over frequency were shown in Fig. 10. As it can be seen, the variation of the total antenna array gain is 1 dB.

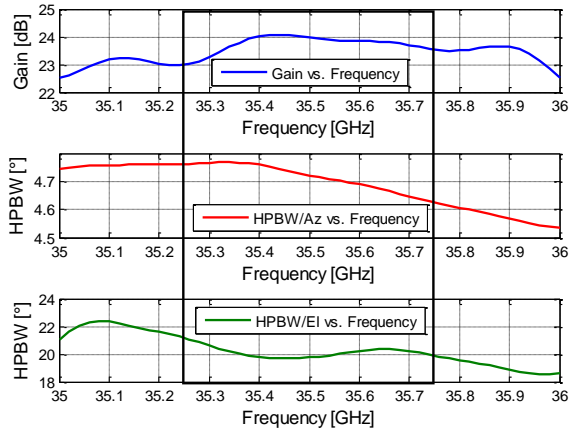


Fig. 10. The measured total gain over the frequency (blue line), the measured half power beam width in azimuth plane θ_{HPBW}/Az over the frequency (red line) and the measured half power beam width in elevation plane θ_{HPBW}/EI over the frequency (green line). The marked area shown the required frequency range.

The half power beam width in the azimuth plane (HPBW/Az) is very stable over the required frequency band. The angle of beam changes only 0.1° . In the elevation plane

(HPBW/EI) a change of 1° is achieved, which still fulfil the specification. However, the presented measurement results confirm that the fabricated antenna array works well within the desired frequency band.

IV. CONCLUSIONS

A horizontally polarized antenna array consisting of four single antenna elements designed in slotted waveguide technology has been introduced in this paper. The use of the transverse slots and the shaped iris pairs caused the radiation. The antenna as well as the feeding network have been fabricated using the erodes technology and assembled by welding device. The final antenna array can provide with its low sidelobe and cross-polarization level, which are 18 dB and 40 dB under the main lobe respectively.

The next step in the development process is to design a corresponding radome, which should protect the antenna from the environmental influences. In order to finish the development of a final dual polarized antenna, a corresponding design of the vertically polarized antenna array is needed as well and it will be done as next.

REFERENCES

- [1] R.Horn, A.Nottensteiner, A.Reigber, J. Fischer and R. Scheiber, "SAR – DLR's new multifrequency polarimetric airborne SAR", IGARSS 2009
- [2] L. Josefsson, S. R. Rengarajan, "Slotted Waveguide Array Antennas", 2018
- [3] R.C.Johnson, "Antenna Engineering handbook, third edition", 1993
- [4] P.Natani, S.Kapoor, C.Saha, S.Kumar, "Design of Slotted Waveguide Array Antenna Fed by H-Plane Power Divider"
- [5] D. Deslandes, F. Boone, K. Wu, "Universal Single-Layer Waveguide Power Divider for Slot Array Antenna Applications", IEEE, 2007
- [6] R.K.Enjiu, M.B.Perotoni, "Slotted Waveguide Antenna Design using 3D EM Simulation", Microwave Journal, July 2013
- [7] Y.Cong, W.Dou, "Design of Dual-Polarized Waveguide Slotted Antenna Array for Ka-band Application", Proceedings of the 9th International Symposium on Antennas, Propagation and EM Theory, January 2011
- [8] R.Tang, "A Slot with Variable Coupling and Its Application to a Linear Array", PGAP, October 1959
- [9] W.Wang, J.Jin, J.Lu, S.Zhong, "An untitled edge-slotted waveguide antenna array design" 38th International Conference on Computational Electromagnetics and Its Applications Proceedings, 2004
- [10] W.Wang, J. Jin, J.-G. Lu, S.-S. Zhong, "Waveguide Slotted Antenna Array With Broadband, Dual-polarization And Low Cross-polarization GFor X-Band SAR Applications", IEEE, 2005
- [11] C.M.Ahsan, Dr.D.Vakula, "Non-inlined slotted waveguide array with various shapes of Irises", International Journal of Advanced Engineering, Management and Science, June 2016
- [12] A. Kosc, M. Limbach, B.Gabler, A.Reigber, "Design of a horizontally polarized slotted waveguide antenna element for an airborne Ka-PolInSAR system", EuMW, 2019
- [13] J. Uher, J. Bornemann, U. Rosenberg, "Waveguide Components for Antenna Feed Systems: Theory and CAD", 1993
- [14] Moghavvemi, M. and A. Mahabadi, H. and A. Farhang, "Multi-Hole Waveguide Directional Couplers", MPRA, 2012
- [15] M. Limbach, B. Gabler, R. Horn, A. Reigber, "DLR-HR Compact Test Range Facility", 3rd European Conference on Antennas and Propagation, 2009

